Chemical Science

EDGE ARTICLE

View Article Online
View Journal | View Issue

Cite this: *Chem. Sci.*, 2019, **10**, 569

All publication charges for this article have been paid for by the Royal Society of Chemistry

Received 12th September 2018
Accepted 18th October 2018

DOI: 10.1039/c8sc04061c

rsc.li/chemical-science

A divergent synthetic pathway for pyrimidine-embedded medium-sized azacycles through an N-quaternizing strategy†

Yoona Choi, ‡ Heejun Kim ‡ and Seung Bum Park*

Medium-sized heterocycles have recently received significant attention because of their potential roles as modulators of protein–protein interactions, but their molecular diversity and synthetic availability are still inadequate to meet the demand. To address these issues, we developed a new divergent synthetic pathway for skeletally distinct pyrimidine-containing medium-sized azacycles. We introduced N-quaternized pyrimidine-containing polyheterocycles as novel key intermediates for diversity-generating reactions *via* selective bond cleavages or migrations and prepared 14 discrete core skeletons in an efficient manner. The skeletal diversity of the resulting molecular frameworks was confirmed by chemoinformatic analysis.

Introduction

The identification of novel bioactive small-molecules is an essential research element in drug discovery and chemical biology. Small-molecule collections with high three-dimensional (3D) skeletal diversity and complexity are invaluable resources in the discovery of new chemical probes or therapeutic agents, especially for regulating protein–protein interactions.[1–3] In this regard, the emergence of diversity-oriented synthesis (DOS) has provided access to unprecedented molecular frameworks with maximized skeletal and stereochemical diversity, which enables an unbiased screening of compounds and discovery of their interactions with diverse biological targets.[4–6] Recently, a variety of divergent synthetic strategies to create discrete core skeletons have been developed.[7] Along with its structural diversity, the biological relevancy of a chemical library is another important consideration for targeting the bioactive chemical space. To satisfy the two criteria simultaneously, we devised a privileged substructure-based DOS (pDOS) strategy based on the assumption that privileged structural motifs could be effective "chemical navigators" to access unexploited biologically relevant chemical space.[8,9] The pDOS strategy focuses on the assembly of discrete heterocyclic moieties around the privileged substructures through divergent synthesis in an efficient manner. In the last decade, the effectiveness of the pDOS strategy has been validated by the discovery of novel small-molecule modulators for various biological activities including anti-neuroinflammatory effects,[10] chondrogenesis-inducing activity,[11] and the inhibition of protein–miRNA interactions.[12]

As a continuation of our endeavour to develop new pDOS strategies, we envisioned that pyrimidines would be excellent navigators toward bioactive chemical space because they have been frequently found in bioactive natural products and extensively studied in medicinal chemistry as nucleoside analogues.[13] Therefore, we developed pDOS pathways, which afforded diverse pyrimidine-embedded 6-[14] and 7-membered[15] azacyclic core skeletons through a variety of pairing strategies based on the synthetic versatility of pyrimidine. From this pyrimidine-containing pDOS library, we identified novel bioactive small molecules that modulated the cellular contents of lipid droplets[16] or inhibited the protein–protein interaction between leucyl-tRNA synthetase (LRS) and Ras-related GTP-binding protein D (RagD).[15]

Herein, we describe a novel pDOS pathway for pyrimidine-fused medium-sized rings with high skeletal diversity and biological relevancy. Although 8- to 11-membered cyclic motifs have been observed in various bioactive natural products, these molecular frameworks are hard to find in the current list of top-selling drugs because of their limited synthetic accessibility and consequent underexposure in drug discovery screening exercises.[17] The classical head-to-tail cyclization of linear precursors to access medium-sized rings is much more difficult than the formation of 5- or 6-membered rings because of entropic and enthalpic factors. In this regard, the selective cleavage of a central C–C single bond or C=C double bond to generate a medium-sized carbocycle from a fused bicyclic precursor has been widely studied as an alternative method to access

CRI Center for Chemical Proteomics, Department of Chemistry, Seoul National University, 1 Gwanak-ro, Gwanak-gu, Seoul 08826, Korea. E-mail: sbpark@snu.ac.kr; Fax: +82-2-884-4025

† Electronic supplementary information (ESI) available. CCDC 1866157 and 1866158. For ESI and crystallographic data in CIF or other electronic format see DOI: 10.1039/c8sc04061c

‡ These authors contributed equally to this work.

medium-sized rings (Fig. 1A).[18] Recently, a series of DOS approaches for medium-sized molecular frameworks using the cleavage of C–C or C=C zero bridges as the main strategy have been reported.[19–21] However, there are limited studies[22–24] on the cleavage of N–N bonds to afford the medium-sized heterocycles, especially those with the potential to interact with biopolymers differently than the analogous carbocycles.

More importantly, the reported methods for the reductive cleavage of N–N bonds are not suitable for diversity-generating reactions. To address this issue, we designed a divergent synthetic pathway for the facile construction of distinct pyrimidine-embedded medium-sized azacycles through chemoselective N–N bond cleavages or rearrangements from N-quaternized key intermediates (Fig. 1B). Fourteen discrete pyrimidine-containing medium-sized azacycles were synthesized and their 3D structural diversity was confirmed by *in silico* analysis.

Results and discussion

Design of diversity-generating pathways for pyrimidine-containing medium-sized azacycles

To prepare diverse pyrimidine-containing medium-sized rings, we first designed key intermediates **1**, prepared by selective N-quaternization of azacyclic precursors derived from the reactions of functionalized pyrimidine moieties with cyclic hydrazines (Fig. 1B). As the polyheterocyclic precursors were designed to have a single tertiary amine whose nucleophilicity would be stronger than those of the other anilinic nitrogen, selective N-quaternization using a variety of alkyl halides was possible. Regarding the quaternized nitrogen as a reaction center, base- and/or hydride-mediated orthogonal transformations into diverse medium-sized azacycles were devised. In pathway (i), co-treatment with base and hydride allowed the selective cleavage of the N–N zero bridge, forming pyrimidine-fused medium-sized diazacycles (scaffold I). The core skeleton was further diversified to rigid tricyclic scaffolds II and III through differentiated ring fusions utilizing the functional groups of scaffold I. Base treatment of intermediate **1** triggered cleavage of the N–N bond followed by

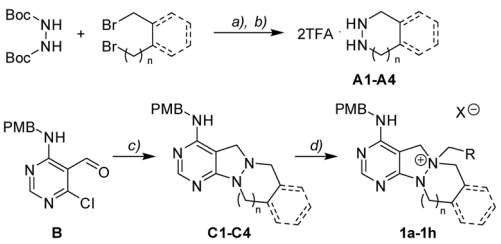

Scheme 1 Synthetic scheme for pyrimidine-containing azacyclic key intermediates **1a–1h**. Reagents and conditions: (a) tetraethylammonium bromide (TEAB), 50% aq. NaOH, toluene/H_2O (2 : 1 v/v), 100 °C; (b) TFA, DCM, r.t.; (c) cyclic hydrazine (**A1–A4**), TEA, EtOH, 80 °C, then $NaBH_4$, EtOH, r.t.; (d) RCH_2X, ACN, 40–80 °C.

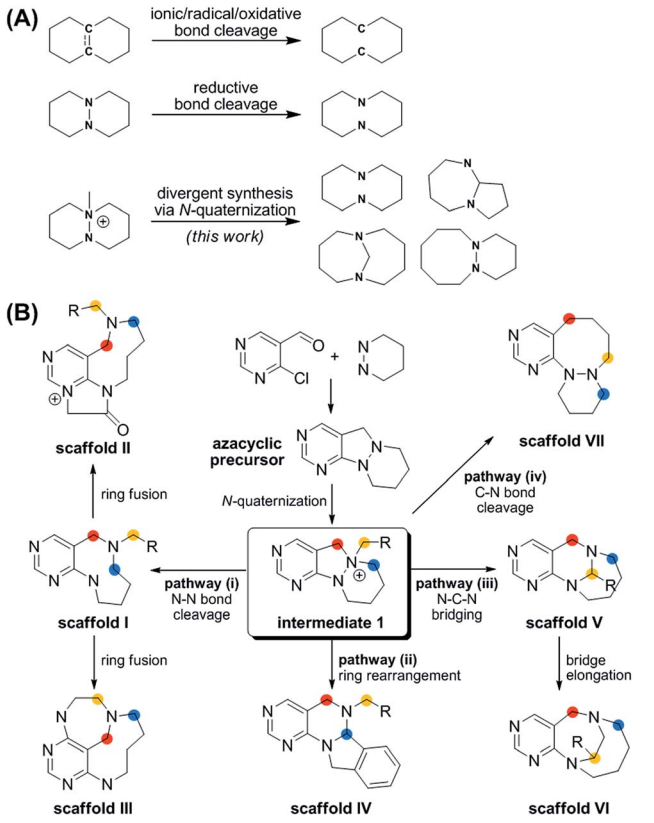

Fig. 1 (A) Synthetic strategies for medium-sized rings *via* ring cleavage. (B) Divergent synthetic pathway for pyrimidine-containing medium-sized azacycles through N-quaternizing strategy.

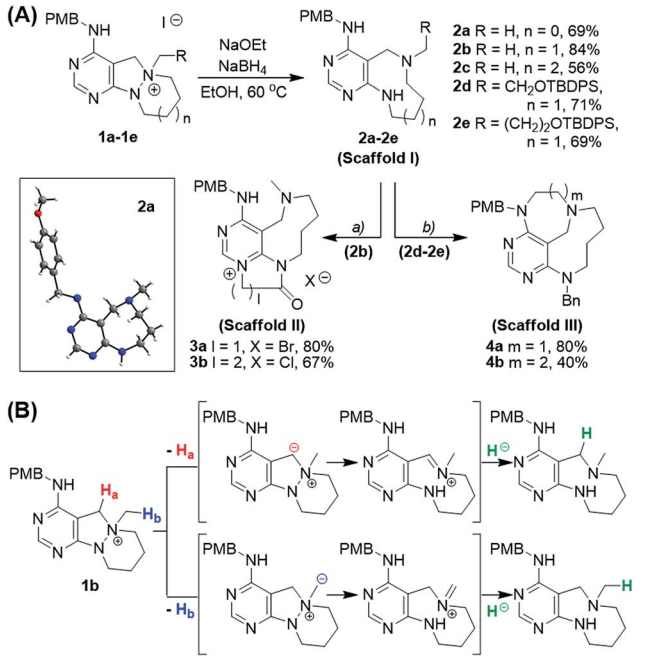

Scheme 2 (A) Exploration of N–N bond cleavage pathway (i) and subsequent ring fusions for scaffolds I–III. Reagents and conditions: (a) bromoacetyl bromide, ACN, 80 °C (for **3a**) or 3-chloropropionyl chloride, DMF, r.t. to 120 °C (for **3b**); (b) BnBr, ACN, then HF/pyridine/THF, then MsCl, DCM, then NaH, DMF, r.t. (B) Proposed mechanism of N–N bond cleavage reaction.

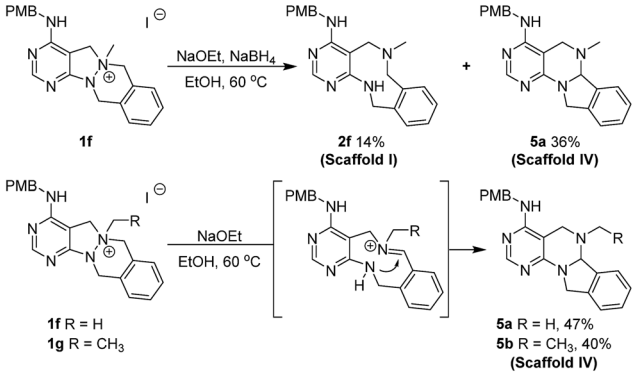

Scheme 3 Exploration of ring-rearrangement pathway (ii) for scaffold IV.

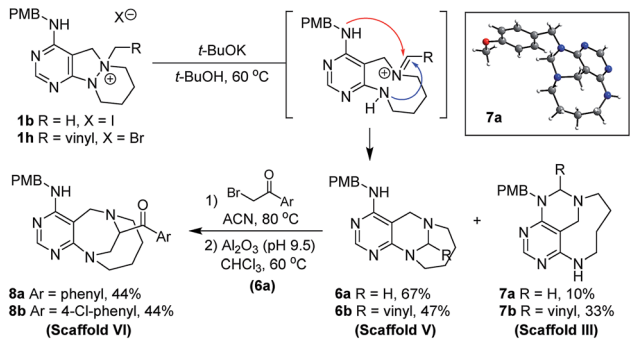

Scheme 4 Exploration of N–C–N bridging pathway (iii) for scaffold V and subsequent bridge elongation for scaffold VI.

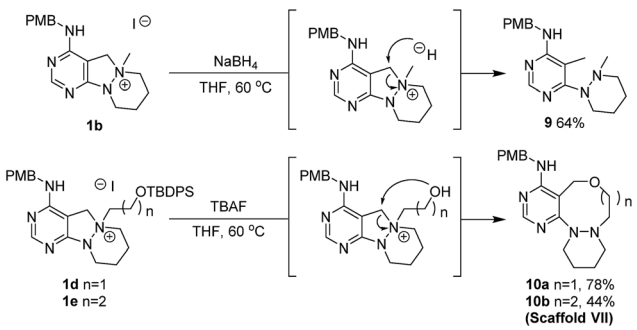

Scheme 5 Exploration of C–N bond cleavage pathway (iv) for scaffold VII.

intramolecular aminal formation to give ring-rearranged scaffold IV *via* pathway (ii) or N–C–N bridged scaffold V *via* pathway (iii). Successive ring expansion from scaffold V allowed the formation of ethano-bridged scaffold VI. Finally, selective C–N bond cleavage without dissociation of the N–N bond afforded medium-sized polyheterocycles (scaffold VII) *via* pathway (iv). Consequently, distinct pyrimidine-embedded medium-sized azacycles with high skeletal diversity were successfully established under precisely controlled reaction conditions.

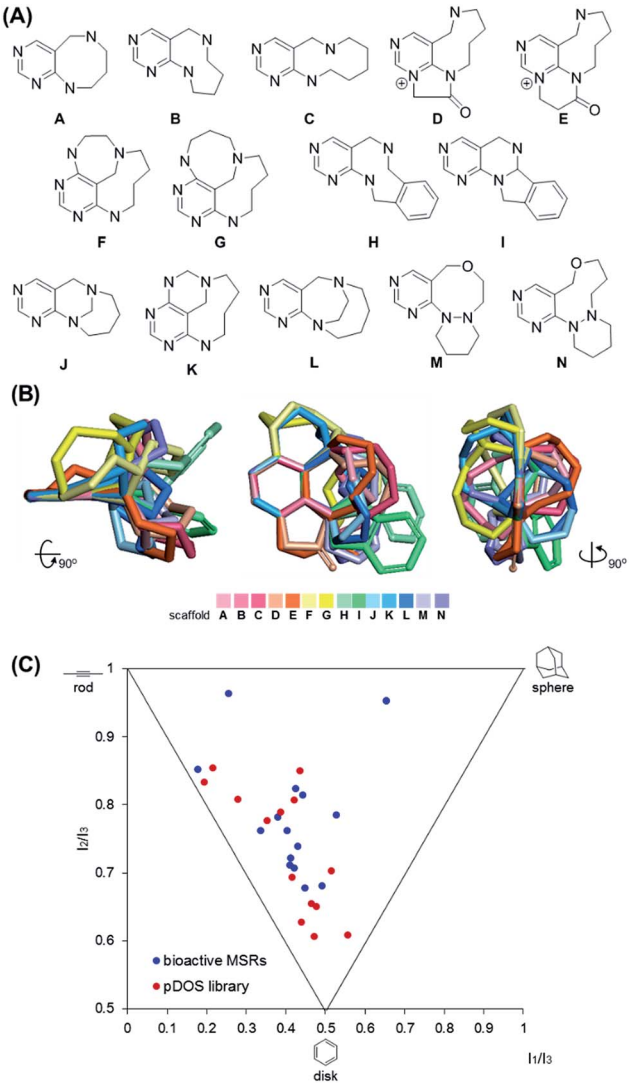

Fig. 2 Chemoinformatic analysis of discrete pyrimidine-embedded medium-sized azacycles. (A) Core skeletons of 14 discrete scaffolds (scaffold I: **A**–**C**, **H**; scaffold II: **D**, **E**; scaffold III: **F**, **G**, **K**; scaffold IV: **I**; scaffold V: **J**; scaffold VI: **L**; scaffold VII: **M**, **N**). (B) Overlay of energy-minimized conformers of 14 core skeletons aligned by the pyrimidine substructure. (C) Principal moment of inertia (PMI) plot. The 3D molecular shapes of pDOS library (red dots) were compared with those of 15 benzannulated medium-sized rings (MSRs) in bioactive natural products and synthetic molecules (blue dots).

Synthesis of pyrimidine-containing key intermediates

To investigate the designed transformations, we prepared pyrimidine-containing azacyclic precursors having a central N–N bond (Scheme 1). First, cyclic hydrazines (**A1**–**A4**) were synthesized from the coupling of di-*tert*-butyl hydrazodiformate with different alkyl dibromides *via* double S_N2 reaction and the subsequent deprotection of the *tert*-butyloxycarbonyl (Boc) groups in the presence of trifluoroacetic acid (TFA). The sequential cyclization and reduction of functionalized pyrimidine (B) with the prepared cyclic hydrazines (**A1**–**A4**) efficiently afforded azacyclic precursors (**C1**–**C4**). Finally, the key

intermediates (**1a–1h**) were prepared through selective N-quaternization of **C1–C4** with various alkyl halides.

Scaffold differentiation studies

Pathway (i). We initiated our investigation of the N–N bond cleavage reaction using **1b** as a substrate. A previous report on the cleavage of an N–N zero bridge through a Hofmann-type elimination from an N-quaternized precursor using NaOMe[24] served as our starting point for optimizing the reaction conditions. After screening a wide range of base, hydride source, and solvent combinations (see ESI† for optimization table), we found that treatment with NaOEt and $NaBH_4$ in EtOH media smoothly transformed the N-quaternized key intermediate **1b** into 9-membered diazonane-fused pyrimidine **2b** in high yield (84%, Scheme 2A). To test the scope of this transformation for further diversification, other intermediates were examined under the optimized conditions. For instance, 8-membered diazocane- and 10-membered diazecane-fused pyrimidines **2a** and **2c** were successfully synthesized from **1a** and **1c**, respectively. The formation of medium-sized azacycles *via* N–N cleavage was clearly confirmed by the structural elucidation of **2a** using X-ray crystallography. Moreover, it is worth mentioning that the N–N bond cleavage reaction conditions were sufficiently mild to produce pyrimidine-fused diazonanes **2d** and **2e** containing functionalized substituents (silyl-protected hydroxyethyl or hydroxypropyl moieties, respectively) for late-stage elaboration.

Although pleased with the outcome of these reactions, we were not confident that the cleavage of the N–N bond occurred *via* the previously reported Hofmann-type β-elimination because the reaction did not occur when using only NaOEt. Moreover, the presence of benzylic protons (H_a), which are more acidic than β-protons, brought the reaction mechanism into question. Therefore, we considered that the N–N bond could be cleaved through the base-triggered formation of an iminium species and its subsequent neutralization by hydride addition (Scheme 2B). To understand the reaction mechanism, we performed a deuterium-labelling experiment with **1b** using $NaBD_4$ to find the site of nucleophilic attack. According to the ^{1}H NMR data, deuterium was introduced into the methyl position (H_b) predominantly compared to the benzylic position (H_a) (see ESI†). Additionally, when NaCN was used as a nucleophile instead of a hydride source, the cyanide-added product in the H_b position was obtained as a major product. On the basis of these results, we proposed a new reaction mechanism for N–N bond cleavage through base-promoted iminium formation followed by hydride-mediated neutralization as shown in Scheme 2B.

Along with the efficient cleavage of the N–N bond, further transformations of scaffold I were demonstrated by utilizing both pre-embedded and newly introduced functionalities (Scheme 2A). The 9-membered diazonane **2b** was treated with dielectrophiles such as bromoacetyl bromide or 3-chloropropionyl chloride, which selectively acylated the newly generated aniline moiety and subsequently cyclized with the pyrimidyl nitrogen to afford scaffold II (**3a** and **3b**) containing a pyrimidinium moiety. In the cases of functionalized diazonanes **2d** and **2e**, we successfully synthesized the conformationally restricted bridged scaffold III (**4a** and **4b**) through an intramolecular substitution reaction using the pre-embedded aniline moiety.

Pathway (ii). In the case of the tetracyclic N-quaternized intermediate **1f**, which has more than one benzylic carbon adjacent to the quaternized nitrogen, the ring-rearranged tetracyclic product **5a** was predominantly obtained compared to the N–N bond cleaved tricyclic product **2f** under the usual reaction conditions for the N–N bond cleavage reaction (Scheme 3). This ring transformation is likely caused by base-promoted iminium formation followed by intramolecular nucleophilic attack of the anilinic nitrogen to form the energetically favorable 6-membered ring, which is preferred compared to the intermolecular hydride attack.[25] Therefore, a new 6/6/5/6-tetracyclic scaffold IV (**5a** and **5b**) could be accessed by the simple base treatment of 6/5/6/6-tetracyclic intermediates (**1f** and **1g**).

Pathway (iii). To generate bridged medium-sized ring scaffold V, we devised an intramolecular reaction that involved the migration of an N–N–C bond to an N–C–N bond. Upon treatment with base (*t*-BuOK) in the absence of a hydride source, **1b** was converted into diazabicyclo[4.3.1]decane-fused pyrimidine **6a**[26] as a major product along with triazabicyclo-[6.3.1]dodecane-fused pyrimidine **7a** as a minor product (Scheme 4). Under the reaction conditions, there are two nucleophiles that could attack the iminium carbon in an intramolecular fashion, so that the formation of both scaffold V (**6a** and **6b**) and scaffold III (**7a** and **7b**) would be possible. The structural identification of **7a** was performed by X-ray crystallography. It is interesting that **6a** and **7a** were obtained in relatively high selectivity (67% and 10% yields, respectively) when the R group was a proton (**1b**), while the selectivity was reduced in the case of a vinyl R group (**6b** and **7b** were obtained in 47% and 33% yields, respectively). In addition, further transformation of the resulting bridged structure **6a** was investigated to afford ethano-bridged diazabicyclo[4.3.2] undecane-fused pyrimidines through bridge elongation. The new homologated bridged azacycles **8a** and **8b** (scaffold VI) were synthesized through the selective N-quaternization of **6a** with α-bromoacetophenone derivatives and the subsequent migration of the α-carbon under mild basic conditions.[27]

Pathway (iv). Different from the former reaction pathways, the treatment of **1b** with $NaBH_4$ in aprotic media without base yielded C–N bond-cleavage product **9** through direct hydride attack at the benzylic carbon (Scheme 5). Using this orthogonal reactivity of the key intermediate **1b**, we devised the synthesis of scaffold VII through internal nucleophile-triggered dissociation of the C–N bond, and designed **1d** and **1e** containing a silyloxy group as a potential nucleophile. Upon treatment with tetrabutylammonium fluoride (TBAF), key intermediates **1d** and **1e** were respectively converted into ring- expanded 8- or 9-membered oxadiazacycles **10a** and **10b** as scaffold VII through removal of the silyl group followed by intramolecular nucleophilic attack of the alkoxide moiety.

Chemoinformatic analysis of the newly synthesized scaffolds

It is worth mentioning that we achieved skeletal diversity among the various medium-sized azacycles through chemoselective bond cleavage or rearrangement *via* the N-quaternizing strategy, while the conventional reductive N–N bond cleavage of cyclic hydrazines using transition metal-catalyzed hydrogenation allows simple cleaved azacycles. With this pDOS pathway, we synthesized 14 discrete core skeletons that contain not only synthetically challenging but also biologically relevant pyrimidine-embedded medium-sized and/or bridged azacycles (Fig. 2A). The constructed chemical library includes unique molecular frameworks such as 8- to 10-membered ring-fused diazacycles (**A–E** and **H**), five different bridged structures (**F**, **G**, and **J–L**), and 8- to 9-membered ring-containing oxadiazacycles (**M** and **N**). To visualize the skeletal diversity of the resulting scaffolds, we determined the energy-minimized conformer of each scaffold using quantum mechanical calculations (see ESI† for detailed procedures). As shown in Fig. 2B, we clearly visualized the skeletal diversity of the 14 scaffolds (**A–N**) by overlaying their calculated 3D structures, aligning their pyrimidine substructure. Furthermore, we performed a principal moment of inertia (PMI) analysis to compare the shape diversity of our pyrimidine-containing medium-sized polyheterocycles with 15 benzannulated medium-sized rings in bioactive natural products and synthetic molecules.[28] As shown in Fig. 2C, a good level of molecular shape distribution was achieved in the polyheterocycles derived from our pDOS library, similar to that of the bioactive medium-sized heterocycles. We also confirmed the good structural diversity of the resulting 14 scaffolds *via* Tanimoto similarity matrix analysis[29,30] (see Fig. S3†).

Conclusions

We developed a new divergent synthetic pathway *via* an N-quaternizing strategy for efficient access to diverse pyrimidine-embedded medium-sized azacycles. Easily accessible N-quaternized key intermediate **1** could be efficiently transformed to 14 discrete scaffolds through chemoselective bond cleavage or migration. The skeletal diversity of each scaffold was demonstrated by structural alignment in 3D space and the PMI analysis of energy-minimized conformers. This unique chemical library of medium-sized azacycles might serve as a valuable resource for the discovery of novel small-molecule modulators and potential therapeutic agents, especially for modulating protein–protein interactions. The biological evaluation of the resulting compound collection will be reported in due course.

Experimental procedures

General synthetic procedure for scaffold I (2a–2f)

To a solution of **1a–1f** (0.16 mmol) in ethanol (3.2 mL, 0.05 M), NaOEt (0.24 mmol) and $NaBH_4$ (1.6 mmol) were added at room temperature. The resulting mixture was stirred at 60 °C. After completion of the reaction (checked by TLC), the reaction mixture was concentrated under reduced pressure, quenched with deionized water and saturated aq. $NaHCO_3$, and the organic material was extracted three times with ethyl acetate (EA). The combined organic extracts were dried over anhydrous Na_2SO_4(s) and filtered. After the solvent was evaporated under reduced pressure, the residue was purified by silica gel flash column chromatography to obtain desired compounds **2a–2f** in moderate to high yields. In the cases of **2d** and **2e**, 3.2 mmol of $NaBH_4$ were used.

General synthetic procedure for scaffold II (3a–3b)

To a solution of **2b** (73.0 mg, 0.23 mmol) in acetonitrile (ACN, 4.6 mL, 0.05 M), either 2-bromoacetyl bromide (for **3a**, 21.4 μL, 0.25 mmol) or 3-chloropropionyl chloride (for **3b**, 24.6 μL, 0.26 mmol) were added at room temperature. The resulting mixture was stirred at 80 °C (for **3a**) or room temperature to 120 °C (for **3b**). After completion of the reaction (checked by TLC), the reaction mixture was concentrated under reduced pressure, and the resulting residue was purified by silica gel flash column chromatography to obtain desired compounds **3a** and **3b** in 80% and 67% yields, respectively.

General synthetic procedure for scaffold III (4a–4b)

Precursors for **4a** and **4b** were obtained through a three-step synthesis including benzylation, desilylation, and mesylation from **2d** and **2e**, respectively (see ESI† for detailed procedures). The prepared precursors (0.051 mmol) and NaH (60% dispersion in mineral oil, 4.1 mg, 0.102 mmol) were dissolved in dry DMF (1.0 mL, 0.05 M) under an argon atmosphere with stirring at room temperature. After completion of the reaction (checked by TLC), the resulting mixture was quenched with deionized water and saturated aq. $NaHCO_3$, and the organic material was extracted three times with EA and three times with DCM. The combined organic extracts were dried over anhydrous Na_2SO_4(s) and filtered. The solvent was evaporated under reduced pressure, and the residue was purified by silica gel flash column chromatography to obtain desired compounds **4a–4b** in moderate to good yields.

General synthetic procedure for scaffold IV (5a–5b)

To a solution of **1f** or **1g** (0.15 mmol) in ethanol (3.0 mL, 0.05 M), NaOEt (51.0 mg, 0.75 mmol) was added at room temperature. The resulting mixture was stirred at 60 °C. After the completion of reaction checked by TLC, the reaction mixture was concentrated under reduced pressure, quenched with deionized water and saturated aq. NaCl, and the organic material was extracted four times with EA. The combined organic extracts were dried over anhydrous Na_2SO_4(s) and filtered. The solvent was evaporated under reduced pressure, and the residue was purified by silica gel flash column chromatography to obtain desired compounds **5a** and **5b** in moderate yields.

General synthetic procedure for scaffold V (6a–6b) and scaffold III (7a–7b)

To a solution of **1b** or **1h** (0.23 mmol) in *tert*-butanol (*t*-BuOH, 4.6 mL, 0.05 M), potassium *tert*-butoxide (*t*-BuOK, 127.2 mg,

1.13 mmol) was added at room temperature. The resulting mixture was stirred at 60 °C. After the standard work-up procedure, the resulting residue was purified by silica gel flash column chromatography to obtain desired compounds **6a–6b** as major products and **7a–7b** as minor products.

General synthetic procedure for scaffold VI (8a–8b)

To a solution of **6a** (0.29 mmol) in acetonitrile (5.8 mL, 0.05 M), 2-bromoacetophenone (for **8a**, 63.2 mg, 0.32 mmol) or 2-bromo-4′-chloroacetophenone (for **8b**, 74.2 mg, 0.32 mmol) was added at room temperature. The resulting mixture was stirred at 80 °C. After complete consumption of the starting material (checked by TLC), the reaction mixture was concentrated under reduced pressure. The residue was dissolved in $CHCl_3$ (11.6 mL, 0.025 M) and basic alumina (Brockmann activity I, pH 9.5 ± 0.5, 400 wt%) was added at room temperature. The resulting mixture was stirred at 60 °C. When TLC indicated completion of the reaction, the reaction mixture was filtered through Celite® while washing with DCM, EA, and MeOH. The filtrate was concentrated under reduced pressure, followed by silica gel flash column chromatography to obtain desired compounds **8a–8b** in moderate yields.

General synthetic procedure for scaffold VII (10a–10b)

To a solution of **1d** or **1e** (0.22 mmol) in tetrahydrofuran (THF, 2.2 mL, 0.1 M), TBAF (1.0 M in THF, 0.33 mL, 0.33 mmol) was added at room temperature. The resulting mixture was stirred at 60 °C. After the standard work-up procedure, the resulting residue was purified by silica gel flash column chromatography to obtain desired compounds **10a** and **10b** in moderate to good yields.

Conflicts of interest

There are no conflicts to declare.

Acknowledgements

This work was supported by the National Creative Research Initiative Grant (NRF-2014R1A3A2030423) and the Bio & Medical Technology Development Program (2012M3A9C4048780) through the National Research Foundation of Korea (NRF) funded by the Korean Government (Ministry of Science and ICT). We acknowledge Ms Jaeyoung Koo for her support in compound crystallization. Y. C. and H. K. are grateful for the BK21 Fellowship Program.

Notes and references

1 S. Dandapani and L. A. Marcaurelle, *Nat. Chem. Biol.*, 2010, **6**, 861–863.
2 D. C. Swinney and J. Anthony, *Nat. Rev. Drug Discovery*, 2011, **10**, 507–519.
3 C. J. O'Connor, L. Laraia and D. R. Spring, *Chem. Soc. Rev.*, 2011, **40**, 4332–4345.
4 S. L. Schreiber, *Nature*, 2009, **457**, 153–154.
5 W. R. J. D. Galloway, A. Isidro-Llobet and D. R. Spring, *Nat. Commun.*, 2010, **1**, 80.
6 C. J. O'Connor, H. S. G. Beckmann and D. R. Spring, *Chem. Soc. Rev.*, 2012, **41**, 4444–4456.
7 (*a*) H. Mizoguchi, H. Oikawa and H. Oguri, *Nat. Chem.*, 2014, **6**, 57–64; (*b*) R. J. Rafferty, R. W. Hicklin, K. A. Maloof and P. J. Hergenrother, *Angew. Chem., Int. Ed.*, 2014, **53**, 220–224; (*c*) J. Zhang, J. Wu, B. Hong, W. Ai, X. Wang, H. Li and X. Lei, *Nat. Commun.*, 2014, **5**, 4614; (*d*) M. Garcia-Castro, L. Kremer, C. D. Reinkemeier, C. Unkelbach, C. Strohmann, S. Ziegler, C. Ostermann and K. Kumar, *Nat. Commun.*, 2015, **6**, 6516; (*e*) F. Nie, D. L. Kunciw, D. Wilcke, J. E. Stokes, W. R. J. D. Galloway, S. Bartlett, H. F. Sore and D. R. Spring, *Angew. Chem., Int. Ed.*, 2016, **55**, 11139–11143; (*f*) Y.-C. Lee, S. Patil, C. Golz, C. Strohmann, S. Ziegler, K. Kumar and H. Waldmann, *Nat. Commun.*, 2017, **8**, 14043.
8 S. Oh and S. B. Park, *Chem. Commun.*, 2011, **47**, 12754–12761.
9 J. Kim, H. Kim and S. B. Park, *J. Am. Chem. Soc.*, 2014, **136**, 14629–14638.
10 S. Lee, Y. Nam, J. Y. Koo, D. Lim, J. Park, J. Ock, J. Kim, K. Suk and S. B. Park, *Nat. Chem. Biol.*, 2014, **10**, 1055–1060.
11 T.-J. Cho, J. Kim, S.-K. Kwon, K. Oh, J.-a. Lee, D.-S. Lee, J. Cho and S. B. Park, *Chem. Sci.*, 2012, **3**, 3071–3075.
12 D. Lim, W. G. Byun, J. Y. Koo, H. Park and S. B. Park, *J. Am. Chem. Soc.*, 2016, **138**, 13630–13638.
13 (*a*) H. R. Lawrence, M. P. Martin, Y. Luo, R. Pireddu, H. Yang, H. Gevariya, S. Ozcan, J.-Y. Zhu, R. Kendig, M. Rodriguez, R. Elias, J. Q. Cheng, S. M. Sebti, E. Schonbrunn and N. J. Lawrence, *J. Med. Chem.*, 2012, **55**, 7392–7416; (*b*) A. E. Wakeling, S. P. Guy, J. R. Woodburn, S. E. Ashton, B. J. Curry, A. J. Barker and K. H. Gibson, *Cancer Res.*, 2002, **62**, 5749–5754; (*c*) V. Yaziji, D. Rodríguez, H. Gutiérrez-de-Terán, A. Coelho, O. Caamaño, X. García-Mera, J. Brea, M. I. Loza, M. I. Cadavid and E. Sotelo, *J. Med. Chem.*, 2011, **54**, 457–471.
14 H. Kim, T. T. Tung and S. B. Park, *Org. Lett.*, 2013, **15**, 5814–5817.
15 J. Kim, J. Jung, J. Koo, W. Cho, W. S. Lee, C. Kim, W. Park and S. B. Park, *Nat. Commun.*, 2016, **7**, 13196.
16 Y. Choi, H. Kim, Y.-H. Shin and S. B. Park, *Chem. Commun.*, 2015, **51**, 13040–13043.
17 N. A. McGrath, M. Brichacek and J. T. Njardarson, *J. Chem. Educ.*, 2010, **87**, 1348–1349.
18 Selected examples: (*a*) P. S. Wharton and M. D. Baird, *J. Org. Chem.*, 1971, **36**, 2932–2937; (*b*) M. C. Honan, A. Balasuryia and T. M. Cresp, *J. Org. Chem.*, 1985, **50**, 4326–4329; (*c*) P. Dowd and S.-C. Choi, *J. Am. Chem. Soc.*, 1987, **109**, 6548–6549; (*d*) H. Suginome, T. Kondoh, C. Gogonea, V. Singh, H. Goto and E. Osawa, *J. Chem. Soc., Perkin Trans. 1*, 1995, 69–81; (*e*) I. J. Borowitz, G. Gonis, R. Kelsey, R. Rapp and G. J. Williams, *J. Org. Chem.*, 1966, **31**, 3032–3037; (*f*) I. J. Borowitz and R. D. Rapp, *J. Org. Chem.*, 1968, **34**, 1370–1373.
19 F. Kopp, C. F. Stratton, L. B. Akella and D. S. Tan, *Nat. Chem. Biol.*, 2012, **8**, 358–364.
20 L. Li, Z.-L. Li, F.-L. Wang, Z. Guo, Y.-F. Cheng, N. Wang, X.-W. Dong, C. Fang, J. Liu, C. Hou, B. Tan and X.-Y. Liu, *Nat. Commun.*, 2016, **7**, 13852.

21 R. A. Bauer, T. A. Wenderski and D. S. Tan, *Nat. Chem. Biol.*, 2013, **9**, 21–29.
22 H. H. Wasserman and H. Masuyama, *J. Am. Chem. Soc.*, 1981, **103**, 461–462.
23 H. Stetter and H. Spangenberger, *Chem. Ber.*, 1958, **91**, 1982–1988.
24 P. Aeberli and W. J. Houlihan, *J. Org. Chem.*, 1969, **34**, 2715–2720.
25 A. Nakamura and S. Kamiya, *Chem. Pharm. Bull.*, 1972, **20**, 69–75.
26 P. Aeberli and W. J. Houlihan, *J. Org. Chem.*, 1969, **34**, 2720–2723.
27 C. Michon, A. Sharma, G. Bernardinelli, E. Francotte and J. Lacour, *Chem. Commun.*, 2010, **46**, 2206–2208.
28 A. Hussain, S. K. Yousuf and D. Mukherjee, *RSC Adv.*, 2014, **4**, 43241–43257.
29 D. J. Rogers and T. T. Tanimoto, *Science*, 1960, **132**, 1115–1118.
30 R. W. Huigens III, K. C. Morrison, R. W. Hicklin, T. A. Flood Jr, M. F. Richter and P. J. Hergenrother, *Nat. Chem.*, 2013, **5**, 195–202.